Adult Restoration of *Shank3* Expression Rescues Selective Autistic-Like Phenotypes

Yuan Mei[1,*], **Patricia Monteiro**[1,2,3,*], **Yang Zhou**[1], **Jin-Ah Kim**[1], **Xian Gao**[1,4], **Zhanyan Fu**[1,3], and **Guoping Feng**[1,3]

[1]McGovern Institute for Brain Research, Department of Brain and Cognitive Sciences, Massachusetts Institute of Technology, Cambridge, MA, USA

[2]PhD Programme in Experimental Biology and Biomedicine (PDBEB), Center for Neuroscience and Cell Biology, University of Coimbra, Coimbra, Portugal

[3]Stanley Center for Psychiatric Research, Broad Institute of MIT and Harvard, Cambridge, MA, USA

[4]Key Laboratory of Brain Functional Genomics (Ministry of Education & Science and Technology Commission of Shanghai Municipality), Institute of Cognitive Neuroscience, School of Psychology and Cognitve Science, East China Normal University, Shanghai 200062, China

Abstract

Because ASD is a neurodevelopmental disorder and patients typically display symptoms before the age of three[1], one of the key questions in autism research is whether the pathology is reversible in adults. Here we investigated the developmental requirement of *Shank3*, one of the most prominent monogenic ASD genes that is estimated to contribute to ~1% of all ASD cases[2–6]. SHANK3 is a postsynaptic scaffold protein that regulates synaptic development, function and plasticity by orchestrating the assembly of postsynaptic density (PSD) macromolecular signaling complex[7–9]. Disruptions of the *Shank3* gene in mouse models have resulted in synaptic defects and autistic-like behaviors including anxiety, social interaction deficits, and repetitive behavior[10–13]. We generated a novel *Shank3* conditional knock-in mouse model and used it to demonstrate that re-expression of the *Shank3* gene in adult led to improvements in synaptic protein composition, spine density and neural function in the striatum. We also provided behavioral evidence that certain behavioral abnormalities including social interaction deficit and repetitive grooming behavior could be rescued, while anxiety and motor coordination deficit could not be recovered in adulthood. Together, these results elucidate the profound impact of post-

Corresponding author's complete contact information: Name: Guoping Feng, Address: McGovern Institute for Brain Research, Department of Brain and Cognitive Sciences, Massachusetts Institute of Technology, MIT, 46-3143A, 43 Vassar Street, Cambridge, MA 02139, Phone: 617-715-4898; 617-715-4920, Fax: 617 324-6752, fengg@mit.edu.
*These authors contributed equally to this work.

developmental activation of *Shank3* expression on neural function and demonstrate certain degree of continued plasticity in the adult diseased brain.

The SHANK3 (ProSAP2) protein is a major scaffolding protein at the excitatory synapse, coordinating the recruitment of many postsynaptic signaling molecules[14–15]. Previous work shows that *Shank3* germline deletion in mice disrupts the protein composition at the postsynaptic density (PSD), reduces neurotransmission efficiency and leads to autistic-like behavior[10–13].

To address whether adult reversal of physiological and behavioral abnormalities in *Shank3* mutant mice is possible, we adopted a genetic method that allows for inducible *Shank3* expression. Because *Shank3* duplication is linked to ADHD and bipolar disorder[5,6,16], it is critical to keep *Shank3* expression within its physiological concentrations to avoid potential confounds. Thus, we generated a novel *Shank3* conditional knock-in mouse by using the Cre-dependent genetic switch (FLEx) strategy[17], which enables the conditional manipulation of the *Shank3* gene at its endogenous genomic locus.

We genetically targeted the PDZ domain due to its role in assembling the scaffold complex in the PSD[14–15] (Fig. 1a, Extended Data Fig. 1). In the absence of Cre, the *Shank3fx/fx* mice function as *Shank3* knockout (KO), and result in the deletion of most major isoforms of SHANK3 including the putative alpha, beta, and gamma bands (Fig. 1b). Similar to abnormalities previously reported on *Shank3* KO mice[10–13], these *Shank3fx/fx* mice showed significant deficits in exploratory behavior (Fig. 1c), anxiety (Fig. 1e), motor deficits (Fig. 1d), and displayed open wound lesions which suggest repetitive grooming behavior[12,18]. In addition, they showed impaired neurotransmission in the dorsal striatum (Fig. 1f–g). These novel *Shank3fx/fx* mice thus recapitulate autistic-like phenotypes, enabling us to investigate the possibility of reversing those deficits in adulthood.

To achieve temporal control of *Shank3* expression, we crossed the *Shank3fx/fx* mice to an inducible CAGGS-CreER mouse line[19] that activates global Cre function upon tamoxifen treatment (Extended Data Fig. 1d, e). When the *Shank3fx/fx:CreER+/−* mice reached 2–4.5 months, we used oral gavage to deliver tamoxifen to ensure efficient Cre-mediated gene restoration (Fig. 2a). All experiments were performed on the following three groups: *Shank3+/+:CreER+/−* treated with tamoxifen (WT), *Shank3fx/fx:CreER+/−* treated with tamoxifen (TM), and *Shank3fx/fx:CreER+/−* treated with corn oil vehicle (KO). Synaptosomal preparations showed that tamoxifen treatment restored the expression of most major SHANK3 isoforms including the alpha and beta isoforms to the wildtype level at synapses (Fig. 2b).

Because SHANK3 is the only SHANK protein family member highly enriched in the striatum, a region strongly implicated in certain behaviors associated with autism[12, 18], mechanistic characterizations were primarily carried out on striatal neurons. We found that the synaptic concentrations of scaffold proteins SAPAP3, Homer1b/c and glutamate receptor subunits NR2A, NR2B and GluA2 were significantly reduced in KO striatal synaptosomal preparations. However, in the TM condition, the synaptic levels of these postsynaptic proteins were significantly increased compared to those in the KO, reaching comparable

levels of the WT(Fig. 2c). This molecular alteration shows for the first time that restoring *Shank3* expression in the adult brain can efficiently recruit major scaffolding and signaling proteins to the synapse and assemble the PSD protein network even after the developmental period.

To investigate whether there were functional changes parallel to molecular repair at synapses, we examined striatal physiology. As expected, the KO showed significantly reduced field population spikes. However, the reduced field responses were rescued to WT levels in the TM condition (Fig. 2d–e). We then performed whole-cell recordings and found that KO mice had reduced mEPSC frequency compared to WT mice. Interestingly, mEPSC frequency was rescued in TM to comparable level of WT group (Fig. 2f). We further measured paired pulse ratio (PPR), AMPAR/NMDAR ratio (Extended Data Fig. 2 and 3), and NR2B/total NMDAR ratio (Extended Data Fig. 2c). We found no differences across genotypes. Overall, these results suggest that a primary defect of striatal physiology in KO mice is the reduced mEPSC frequency, and this defect can be improved by restoring Shank3 expression in adulthood.

Previous studies have shown that *Shank3* manipulation can lead to significant changes in the total spine density[6,12]. It is, however, unclear whether post-developmental *Shank3* expression can also affect spine structure. To address this, we used systemic viral injection to sparsely label neurons with GFP in the WT, KO, and TM mice and analyzed their dendritic spines in the dorsal striatum. Similar to our previous report on *Shank3B* KO mice[12], we observed a significant reduction of MSN spine density in the KO compared to the WT. Surprisingly, the total spine density was significantly increased in the TM treated mice compared to the KO mice (Fig. 2g). To our knowledge, this is the first indication that the ability of *Shank3* to promote spine formation or maintenance is not restricted to any developmental critical period, highlighting the continued structural plasticity in the adult striatum. Interestingly, the spine density in the TM condition is significantly higher than that of the WT. One possibility for this phenomenon is that adult *Shank3* expression induces dendritic spines that may not be pruned and regulated by the same processes that occur in development.

We next tested how adult Shank3 expression may affect behavioral abnormalities. Since striatal defects have been strongly linked to repetitive/compulsive behaviors[21] and *Shank3* KO mice show overgrooming[12], we videotaped WT, TM, and KO mice after treatment, and quantified their grooming time. The results indicated that while there was a significant increase in the percentage of time spent grooming in the KO mice compared to WT mice, TM mice exhibited significantly reduced grooming time (Fig. 3a, b). In addition, during the tamoxifen treatment, we noticed that some *Shank3^{fx/fx}:CreER^{+/−}* mice that initially developed lesions began to heal and regrow their lost fur, providing further support that repetitive/excessive grooming phenotype is reversible in the *Shank3^{fx/fx}* mice.

One of the defining features of autism is the impairment in social interaction. Thus, we used a modified three-chamber assay to probe voluntary social interaction[12,13,22]. After habituating to the three-chamber box, the test mice were given a choice of either interacting with a novel object or a stranger mouse. We found that while WT mice demonstrated strong

preference for the stranger mouse over the novel object, KO mice displayed no such preference (Fig. 3c, d). Interestingly, we found that TM mice behaved similarly to their WT controls in that they show strong preference for the stranger mouse in both duration and frequency of interaction (Fig. 3c, d). These data show that, similar to repetitive grooming behavior, social interaction deficit can also be rescued in adulthood. Currently, the neurobiological mechanisms of social deficits of ASD are not well understood. Although ventral striatum has been associated with social interaction[23], we did not observe differences in measurements of mEPSCs, AMPAR/NMDAR ratio, and PPR in the ventral striatum/ nucleus accumbens across genotypes (Extended Data Fig. 4).

Encouraged by the rescue of repetitive grooming and social deficits, we ran a battery of other tests to assess the extent of behavioral rescue. In contrast to the social and grooming behaviors, adult *Shank3* re-expression has minimal impact on reduced locomotion, anxiety-like behavior and motor coordination deficits (Fig. 4). In the open field, TM mice showed no significant difference from the KO mice in exploratory behavior (Fig. 4a) and anxiety-like behavior including rearing time and rearing frequency (Fig. 4b). This result was further corroborated by our observations from the elevated zero maze test (Fig. 4c). In addition, we found no significant recovery in motor coordination deficit (Fig. 4d).

Because the cortex and cerebellum have been linked to anxiety and motor coordination, we assessed the mechanistic changes in these brain regions[24–25]. In both regions, SHANK3 expression was restored to WT level in TM mice (Extended Data Fig. 5 and 6). However, we found minimal differences across the genotypes (Extended Data Fig. 5–7). Thus, the circuit mechanisms of anxiety and motor coordination deficits in the *Shank3* KO mice may involve other brain regions or could be the collective consequence of connectivity deficits across many brain regions.

To address whether the lack of rescue in these behavior phenotypes is indeed due to missing SHANK3 expression during development, we crossed *Shank3*[fx/fx] mice to β-actin-Cre mice, enabling germline restoration of *Shank3*. The germline rescue (GR) mice showed no significant differences in striatal physiology (Extended Data Fig. 4 and 8), exploratory behavior (Fig. 4e), anxiety (Fig. 4f, g), and motor coordination (Fig. 4h) from their wildtype littermates, indicating that restoring *Shank3* expression at the germ cell stage can restore all behavioral phenotypes. Together, these data strongly suggest that there are certain developmental defects that are irreversible by adult re-expression of *Shank3*.

To test whether there is a developmental window for rescuing anxiety and motor deficits, we treated P20–21 mice with tamoxifen to efficiently induce *Shank3* expression (Extended Data Fig. 9a), and assayed their behaviors in adulthood (Extended Data Fig. 9 and 10). As previously reported[26], we observed that treatment of young mice with tamoxifen leads to some toxicity including reduced body weights in the WT mice and affected their motor coordination compared to the KO fed with corn oil (Extended Data Fig. 10d). However, even with the TM toxicity, we found that on the rotarod, the developmentally treated TM mice performed significantly better than their KO counterparts (Extended Data Fig. 10a, b). The P20–21 treated TM mice also showed significantly reduced anxiety on the elevated zero maze compared to the KO mice (Extended Data Fig. 9f). Overall, these behavioral results

showed that earlier intervention yields more behavioral improvement than adult treatment, further supporting the developmental origin of the behavioral abnormalities that are irreversible in adults.

In the current study, we showed for the first time that in the adult mouse brain, *Shank3* expression can increase dendritic spine density, restore the PSD protein composition, and improve striatal neurotransmission. Though adult gene rescue characterizations have been performed on other autism genes[27–28], this is the first report to show selective rescue in specifically autism-related behavioral phenotypes. Importantly, we also demonstrated that the behavioral deficits that are irreversible in the adult can be improved with early postnatal intervention. Our results highlight the unique behavioral impact of Shank3 expression after development, and underscore the surprising extent of continued neural plasticity in the adult brain.

Full Methods

Generation of *Shank3CKI*

The *Shank3^{fx/fx}* targeting vector was designed by inverting the PDZ domain (exons 13 to 16) and flanking it with the FLEx cassette, which is composed of one pair of LoxP sites staggered with one pair of Lox2722 sites. *Shank3^{fx/fx}* conditional knock-in mice were generated by homologous recombination in R1 embryonic stem cells and implanting the correctly targeted cells in C57 blastocysts using standard procedures. Correct locus insertion of the targeting construct into the genomic DNA was determined by PCR genotyping using two primers End_F (5′-GGCAGACTCCACACAGTTCCTG-3′) and LoxR (5′-GTATCCTATACGAAGTTATTCCGGGTCGAC-3′). Subsequent mouse genotyping was determined by PCR of mouse tail or ear DNA using three primers. For the wildtype (WT) allele, primer FuncF2 (5′-CGTTTGACACACATAAGCACC-3′) and primer FuncFlipR4 (5′-CTCCACCTAGCTGAATTTCCC-3′) were used to produce a band of 340 bp. For the knockout (Fx) allele, primer FuncF2 (5′-CGTTTGACACACATAAGCACC-3′) and primer Gen_Flx_R1 (5′-GCTGACATCACATTGCTGCC-3′) were used to produce a band of 481 bp. For the rescue allele, primer FuncF2 (5′-CGTTTGACACACATAAGCACC-3′) and primer FuncFlipR4 (5′-CTCCACCTAGCTGAATTTCCC-3′) were used to produce a band of 408 bp.

Chimeric males were crossed to C57BL/6J females from Jackson Labs. The F1 hybrids were crossed with C57BL/6J β-Actin Flp to remove the Neomycin cassette. All progeny were bred onto the pure C57BL/6J (Jackson Labs) for at least two generations before being bred onto a mixed background with 129S1/SvlmJ (Jackson Labs). Heterozygotes were initially bred with heterozygotes to produce experimental animals. All germline *Shank3^{fx/fx}* (KO) and germline rescue (GR) mice along with their respective wildtype littermates were produced by breeding heterozygotes with heterozygotes. For the adult *Shank3* rescue experiments, the *Shank3* conditional knock-in line was crossed with CAGGS-CreER[19]. In order to produce enough animals for all necessary experiments, breeding strategy was switched to heterozygotes crossed with homozygotes and homozygotes crossed with homozygotes for all conditions (*Shank3^{fx/+}:CreER^{+/−}* bred with *Shank3^{fx/fx}:CreER^{−/−}*; *Shank3^{fx/fx}:CreER^{+/−}* bred with *Shank3^{fx/fx}:CreER^{−/−}*; *Shank3^{+/+}:CreER^{+/−}* bred with

$Shank3^{+/+}$:$CreER^{-/-}$; $Shank3^{+/-}$:$CreER^{+/-}$ bred with $Shank3^{+/+}$:$CreER^{-/-}$). It should be noted that all animals in the rescue condition were produced from the same litters as the animals in the knockout condition. The animals were randomly assigned to different conditions. No computerized randomization program was used.

Animals were housed by genotype at a constant 23°C in a 12 h light/dark cycle (lights on at 07:00, lights dark at 19:00) with ad libitum food and water. Rescue treatment i.e. tamoxifen feeding was initiated on mice at 2–4.5 months. All electrophysiological and behavioral experiments were done at least 6 weeks after treatment in adult mice with the experimenter being blinded to the genotypes. Only age-matched male mice were used for behavioral assays. All experimental procedures were inspected and approved by the MIT Committee on Animal Care.

Open Field

An automated Omnitech Digiscan apparatus (AccuScan Instruments) was used to assess spontaneous locomotion as previously described[21]. Anxiety-like behaviors were assessed by the following parameters: time spent rearing and frequency of rearing. Locomotion was evaluated by the total distance traveled. The first 30 minutes were evaluated for all parameters. Statistical analysis was done using one-way ANOVA with Bonferroni multiple comparison tests.

Zero Maze

An elevated zero maze was illuminated such that the open arm was lit by 60 lux, and the dark arm was lit by 10–20 lux. Animals were habituated with 10–20 lux for at least one hour before test. The animal was introduced into the closed arm and allowed to freely explore the maze for 5 minutes, which was videotaped. An observer blinded to the genotype performed analysis using an automated tracking software Noldus Ethovision. Anxiety-like behavior was assessed by the percentage of time spent by the animal in the open arm during the 5-min interval. Statistical analysis was done using one-way ANOVA with Bonferroni multiple comparison tests.

Rotarod

Animals were placed on a rotarod apparatus (Med Associates) that accelerates 4–40 rpm for 5 minutes. Each animal was tested for three trials with 1–2 hours between trials in a single day. All trials were videotaped. Latency to fall was manually analyzed for each trial on Noldus Observer by an observer blinded to genotypes. The change in the latency to fall over the course of three trials indicates the quality of motor coordination. Statistical analysis was done using two-way repeated measures ANOVA with Bonferroni post-hoc tests.

Grooming

Animals were individually placed into a new cage and allowed to habituate. Grooming behavior was videotaped for 2 hours from 19:00 to 21:00 with red light (2 lux). An observer blinded to the genotype manually quantified grooming behavior using Noldus Observer. All instances of face-wiping, scratching/rubbing of head and ears, and full-body grooming were

counted as grooming behavior. Statistical analysis was done using one-way ANOVA with Bonferroni multiple comparison tests.

Social Interaction

A modified version of the three-chamber social interaction assay was used as previously described[12,13,22]. Only age-matched males were used for all tests. S129 males were used as stranger mice and were habituated to the test chamber for 3 sessions (20 minutes each) one or two days prior to the behavioral assay. On the day of the test, both test and stranger animals were habituated to the test room for at least one hour before the start of the assay. The left and right chamber of the three-chamber apparatus were both lit by 4–6 lux during the test session. Each test animal was first placed into the center chamber with open access to both the left and right chamber, each of which contained an empty wired cup placed upside down. This allowed the animal to habituate to not only the social apparatus, but also the cups that will eventually contain the stranger mice. After 15 minutes of habituation, the test animal was moved back to the center chamber briefly before the next session. During the social phase, an age-matched stranger mouse was placed randomly into one of the two side chambers while a novel object was placed into the other side chamber. The test animal was allowed to freely explore the social apparatus and demonstrate whether it prefers to interact with the novel object or the novel mouse. This social phase was also 15 minutes. The placement of the stranger mouse and the object was alternated between test mice to eliminate any confounds due to chamber bias. Time spent by the test animal in close proximity (~5 cm) to the cup containing either the stranger or the object was calculated. Analysis was done by an observer blinded to the genotype on Noldus Ethovision. One-way ANOVA with Bonferroni *post hoc* test was used for statistical analysis.

Tamoxifen Preparation and Feeding

Tamoxifen (Sigma #T5648) was dissolved in corn oil at 20 mg/ml through vortexing. Freshly prepared tamoxifen was protected from light by aluminum foil and kept for 2–3 days at room temperature. Animal feeding needles from Harvard Apparatus (cat #52-4025) were used for oral gavage. To avoid toxicity of tamoxifen, the following dosages were used for adult animals:

> Mice at 17–21 g body weight were fed 5 mg/day
>
> Mice at 22–25 g body weight were fed 6 mg/day
>
> Mice at 26–29 g body weight were fed 7 mg/day
>
> Mice at 30–35 g body weight were fed 8 mg/day

The adult animals were fed for 5 consecutive days followed by two weeks of rest. Then the animals were fed for 5 more consecutive days followed by another two weeks of rest. Corn oil was fed as a control. The mice fed with tamoxifen and mice fed with corn oil were housed separately to avoid contamination. For induction of Shank3 expression in P20–P21 animals, mice that weighed 7–9 g received 0.1 ml of tamoxifen or corn oil per day for two to three consecutive days. Mice that weighed 10–12 g received 0.15 ml of tamoxifen or coil per day for two to three consecutive days.

Western blot

PSD and synaptosomal fractions of the striatum, cortex, and cerebellum were prepared as previously described[21]. Purified fractions were separated on SDS-PAGE and quantified using Odyssey Licor. β-Actin and Tubulin were used as loading controls. Specific primary antibody for SAPAP3 was prepared as previously described[21]. Commercial antibodies used include SHANK3 (Santa Cruz SC-30193), GluR1 (Millipore MAB2263), GluR2 (Neuromab 75-002), NR1 (BD Biosciences 556308), NR2A (Millipore 07-632), NR2B (Millipore 05-920), Homer1 (Chemicon AB5877, Synaptic Systems 160022), Homer3 (Synaptic Systems 160303), mGLUR5 (Abcam ab76316), CaMKIIa (Millipore 05-532), Shank1 (Synaptic Systems 162002), Shank2 (Cell Signaling 12218S), B-Actin (Sigma A5441), and Tubulin (Sigma T5168). Statistical analysis was done using two-tailed Students' t-tests.

Dendritic Spine Analysis

Mice from WT (N=5), KO (N=4, 1 had to be euthanized due to lesion development), and TM (N=5) conditions at 6 to 12 months old, age-matched males were used. The pAAV-hSyn1-EGFP-P2A-EGFPf-WPRE-HGHpA construct was cloned and sent for commercial viral packaging by Upenn Viral Core with serotype 2/9. Farnesylated GFP (GFPf) was previously shown to target the membrane[29]. To achieve sparse labeling, ~8–30 μL of this virus with titre of 4.04×10^{13} (GC/ml) was injected through the retro-orbital route into each mouse. Three weeks after viral injection, the mice were transcardially perfused with 4% paraformaldehyde and sectioned into 200 micron slices. Immunohistochemistry was performed by staining the slices with anti-GFP antibody (Invitrogen A11122) for 48 hours and 24 hours of secondary antibody incubation. The stained slices were then surrounded by a 240-um depth spacer (Electron Microscopy Sciences) and mounted with Vectashield Mounting Media.

Confocal images were taken with a 60X objective of the dorsal striatum. Spine count on intact neurons began 30–40 μm away from the soma and was extended for 10–60 μm from the origin. Spine density was analyzed automatically by Neuron Studio. All virus injections, imaging, and software analysis were done with the experimenter blinded to the mouse genotypes. Statistical analysis was done using one-way ANOVA, Newman-Keuls post-hoc test.

Electrophysiology slices

Dorsal and ventral striatum—Acute striatal slices were prepared from 3–7 months old age-matched mice. Animals were anesthetized by avertin intraperitoneal injection (tribromoethanol, 20mg/ml, 0.5mg/g body weight) and transcardially perfused with ice-cold oxygenated NMDG-based cutting aCSF solution (mM): 92 N-methyl-D-glucamine (NMDG), 2.5 KCl, 1.20 NaH_4PO_4, 30 $NaHCO_3$, 20 HEPES, 25 glucose, 2 thiourea, 5 Na-ascorbate, 3 Na-pyruvate, 0.5 $CaCl_2$, 10 MgSO4 (~300mOsm, 7.2–7.4pH). Following decapitation, brains were removed for sectioning in the same ice-cold cutting aCSF using a Vibratome 1000 Plus (Leica Microsystems, USA). For all dorsal striatal recordings, 300 μm coronal slices were prepared, unless otherwise stated (Extended Data Fig. 3). For all NAc core recordings, 300 μm parasagittal slices were prepared and NAc core was identified by the presence of anterior commissure. Slices were recovered in the same cutting aCSF

solution at 32°C for 12 min and transferred to room-temperature carbogenated regular aCSF(mM): 119 NaCl, 2.5 KCl, 1.2 NaH_2PO_4, 24 $NaHCO_3$, 12.5 glucose, 2 $MgSO_4.7H_2O$, 2 $CaCl_2.2H_2O$ (~300mOsm, 7.2–7.4 pH). Slices were allowed to recover at least 1h and transferred to a recording chamber (RC-27L, Warner Instruments) prior to recordings. Stimulations were performed using a platinum iridium concentric bipolar electrode (CBAPC75, FHC). For dorsolateral striatum coronal slices, electrode was placed at the corpus callosum to mainly stimulate corticostriatal axons. For dorsolateral striatum parasagittal slices, stimulating electrode was placed at the cortex between layer V and VI. For ventral striatum parasagittal slices, electrode was placed dorsally to the anterior commissure at the border between NAc core and the cortex. Afferents were stimulated with 0.1ms stimulation step (Isoflex, AMPI) delivered at 0.05 Hz frequency (unless otherwise stated). Slices were visualized under IR-DIC (infrared-differential interference contrast) using a BX-51WI microscope (Olympus). All slice preparations, recordings and data analysis were performed with experimenter blinded to the genotypes.

Medial prefrontal cortex (mPFC)—Acute brain slices were prepared from 3–7 month-old mice as follows. Briefly, mice were deeply anesthetized by intra-peritoneal injection of avertin solution (20 mg/ml, 0.5 mg/g body weight) and then transcardially perfused with 20 ml of carbogenated (95% O_2, 5% CO_2) ice cold cutting solution with the composition (in mM): 105 NMDG, 105 HCl, 2.5 KCl, 1.2 NaH_2PO_4, 26 $NaHCO_3$, 25 Glucose, 10 $MgSO_4$, 0.5 $CaCl_2$, 1 L-Ascorbic Acid, 3 Sodium Pyruvate, 2 Thiourea (pH 7.4, with osmolarity of 300–310 mOsm). The brains were rapidly removed and placed in ice-cold and oxygenated cutting solution. Coronal slices (300 μm) were sliced using Leica VT1200S (Leica Microsystems) and then transferred to recovery chamber at 32 °C with carbogenated cutting solution for 8 min, followed by transferring to holding chamber containing aCSF that contained (mM): 119 NaCl, 2.3 KCl, 1.0 NaH_2PO_4, 26 $NaHCO_3$, 11 Glucose, 1.3 $MgSO_4$, 2.5 $CaCl_2$ (pH was adjusted to 7.4 with HCl, with osmolarity of 300–310 mOsm) at room temperature. Slices were allowed to recover for at least two hours in holding chamber before recording and used for experiment typically between 3~7 hours after slicing. Layer 5 pyramidal cells with a prominent apical dendrite were visually identified with a microscope equipped with IR-DIC optics (BX-51WI, Olympus) mainly by location, shape and pClampex online membrane test parameters.

Extracellular field recordings

Slices were prepared from a daily group of mice containing all the 3 genotypes/treatments on randomized order, and recordings were obtained at RT with carbogenated regular aCSF (~2 ml/min rate). Borosilicate glass recording microelectrodes (King Precision Glass) were pulled on a P-97 horizontal puller (Sutter Instruments) and backfilled with 2 M NaCl. Recording electrode was placed ~400 μm away from stimulating electrode and field population-spike was evoked by a 0.1ms stimulation step (Isoflex, AMPI) delivered at 0.05Hz frequency. Input-output functions were generated through consecutive rounds from 0.1–1.0 mA in 0.1 mA increments (triplicate measurements *per* stimulation intensity). Three components were resolved in the recording traces: stimulation artifact, negative peak 1 (NP1, presynaptic fiber volley) and field population spike. Amplitude for each component was determined by the average peak amplitude from triplicated measurements *per*

stimulation intensity. Data was amplified using a MultiClamp 700B and sampled at 10 KHz using a Digidata 1440A acquisition system. Analysis was performed blinded to genotype using pCLAMP 10 software (Axon Instruments/Molecular Devices).

Whole-cell recordings

Borosilicate glass recording microelectrodes (King Precision Glass) were pulled on a P-97 horizontal puller (Sutter Instruments) and backfilled with CsGlu (mM: 110 CsOH, 110 D-Gluconic acid, 15 KCl, 4 NaCl, 5 TEA-Cl, 20 HEPES, 0.2 EGTA, 5 Lidocaine N-ethyl chloride, 4 MgATP, 0.3 NaGTP). Internal pH was adjusted to ~7.3 with KOH and osmolarity adjusted to ~300 mOsm with K_2SO_4. Typical internal resistance was around 3–5 MΩ. MSNs were visually identified based on their shape, size and location under IR-DIC (infrared-differential interference contrast), using a BX-51WI microscope (Olympus). After seal rupture and internal equilibrium (5min to allow proper dialysis of Cs+ internal), cells were recorded with series-resistance values < 20 MΩ (recording traces were excluded for data analysis if Rs changed by >20%). All voltage clamp traces were recorded in the presence of 50 μM PTX (picrotoxin, Tocris) with theoretical liquid junction potential not corrected-for. Signals were filtered at 2 KHz, digitized at 10 KHz and data acquired using a MultiClamp 700B amplifier and a Digidata 1440A. All analyses was performed blinded to the genotype. Grubb's test was used to remove single outliers.

Miniature EPSCs—Slices were perfused with RT carbogenated regular aCSF at a rate of approximately 2 ml/min. Voltage clamp traces were recorded at holding potential −70 mV in the presence of 50 μM PTX (picrotoxin, Tocris), 50 μM DL-APV (DL-2-amino-5-phosphonovaleric acid, Abcam) and 1 μM TTX (tetrodotoxin, Tocris). Analysis of miniature EPSCs was performed using pCLAMP10 (Axon Instruments, Molecular Devices) and Minianalysis software (Synaptosoft Inc, USA) by manually clicking of individual events.

Paired-pulse ratios—Slices were perfused with carbogenated regular aCSF at ~30 °C, ~2 ml/min rate. Stimulus intensity was set to evoke 150–400 pA EPSC at holding potential −70 mV. Two EPSCs (inter-stimulus interval of 50 ms) were evoked for 10 consecutive traces. PPR was calculated by dividing the second EPSC peak amplitude by the first one.

AMPAR/NMDAR ratios—Slices were perfused with carbogenated regular aCSF at ~30 °C, ~2 ml/min rate. Stimulus intensity was set to evoke 150–400 pA EPSC at holding potential −70 mV. An average EPSC was obtained (~10 traces) at −70 mV and then at +40 mV. AMPAR/NMDAR ratio was calculated as the ratio of the average EPSC peak amplitude at −70 mV (AMPAR EPSC) to the average amplitude of the EPSC recorded at +40 mV, 50 ms after afferent stimulation. For pharmacologically isolated AMPAR/NMDAR ratios, dual-component evoked EPSC at +40 mV was recorded before and after DL-APV bath application (50 μM, Abcam). NMDAR EPSC was obtained by digitally subtracting the average EPSC amplitude after APV application (AMPAR EPSC). For NR2B/total NMDAR ratio, dual-component evoked EPSC at +40 mV was recorded before and after ifenprodil bath application (3 μM, NR2B antagonist, Tocris) and ifenprodil blockable fraction was defined as NR2B EPSCs. DL-APV (50 μM) was then applied to block all NMDARs for measuring total NMDAR EPSCs. The fraction of NR2B containing NMDAR EPSCs is

presented as the percentage of the total NMDAR EPSCs (NR2B/total NMDAR ratio = ifenprodil sensitive current divided by DL-APV sensitive current).

Statistical Analyses

All statistical analyses were performed using Prism (GraphPad Software). All data sets were analyzed using D'Agostino-Pearson omnibus test and Shapiro-Wilk test for normality. Data sets with normal distributions were analyzed for significance using either unpaired Student's two-tailed *t*-test or ANOVA measures with multiple comparison post-hoc test, using *P< 0.05, **P<0.01, ***P< 0.001; all data presented as means ± s.e.m. Data sets with non-normal distributions were analyzed using Kruskal-Wallis test with adjustments for multiple comparisons. Based on previously published literature on Shank3 models[10–13], we chose similar sample sizes for all experiments performed. All behavior test results for the tamoxifen treated cohorts are the combination of at least two different large animal cohorts that showed the same results. All electrophysiological, biochemical, and morphological data were obtained by counterbalancing experimental conditions with controls. Further details on particular statistical analyses can be found on the respective figures/results section for each data set.

Extended Data

a

b

c

d
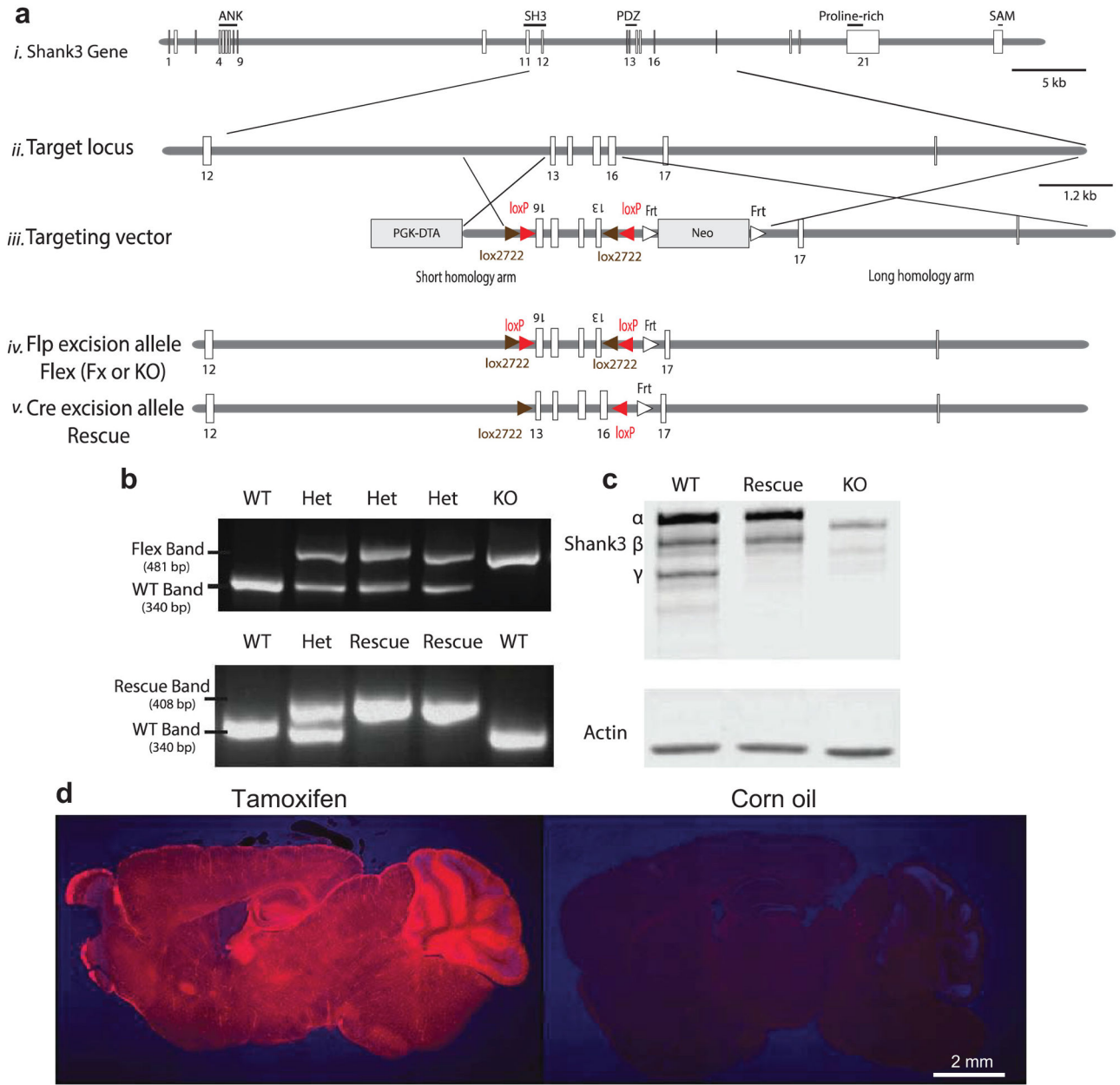
Extended Data Figure 1. Generation of Shank3 conditional knock-in mice
a*i–ii*, Schematic of the Shank3 gene and the target locus. **a***iii*, Targeted exons 13–16. **a***iv*,
Neo-cassette excision via breeding with germline Flp mice. **a***v*, Exons 13–16 re-inversion
via Cre-expressing mice. **b**, PCR genotyping showing the bands for Fx, Rescue, and WT. **c**,
Western blot showing rescue of SHANK3 expression upon germline Cre recombination,
with the exception of putative Shank3g isoform. This is likely due to the disruption of a
putative intronic promoter by the introduction of the LoxP sites. **d,** Tamoxifen-inducible Cre
strategy leads to broad reporter expression. Sagittal sections from pCAGGS-CreER$^{+/−}$;Rosa-
floxstop-tdTomato$^{+/−}$ mice after feeding with tamoxifen (left panel) or corn oil (right panel).

Results show widespread induction of tdTomato reporter expression upon tamoxifen-induced Cre activation but not in the absence of Cre activity (corn oil feeding); pCAGGS promoter consists of the CMV early enhancer with chicken b-actin promoter[19]. See Supplementary Figure 1 for gel source data.
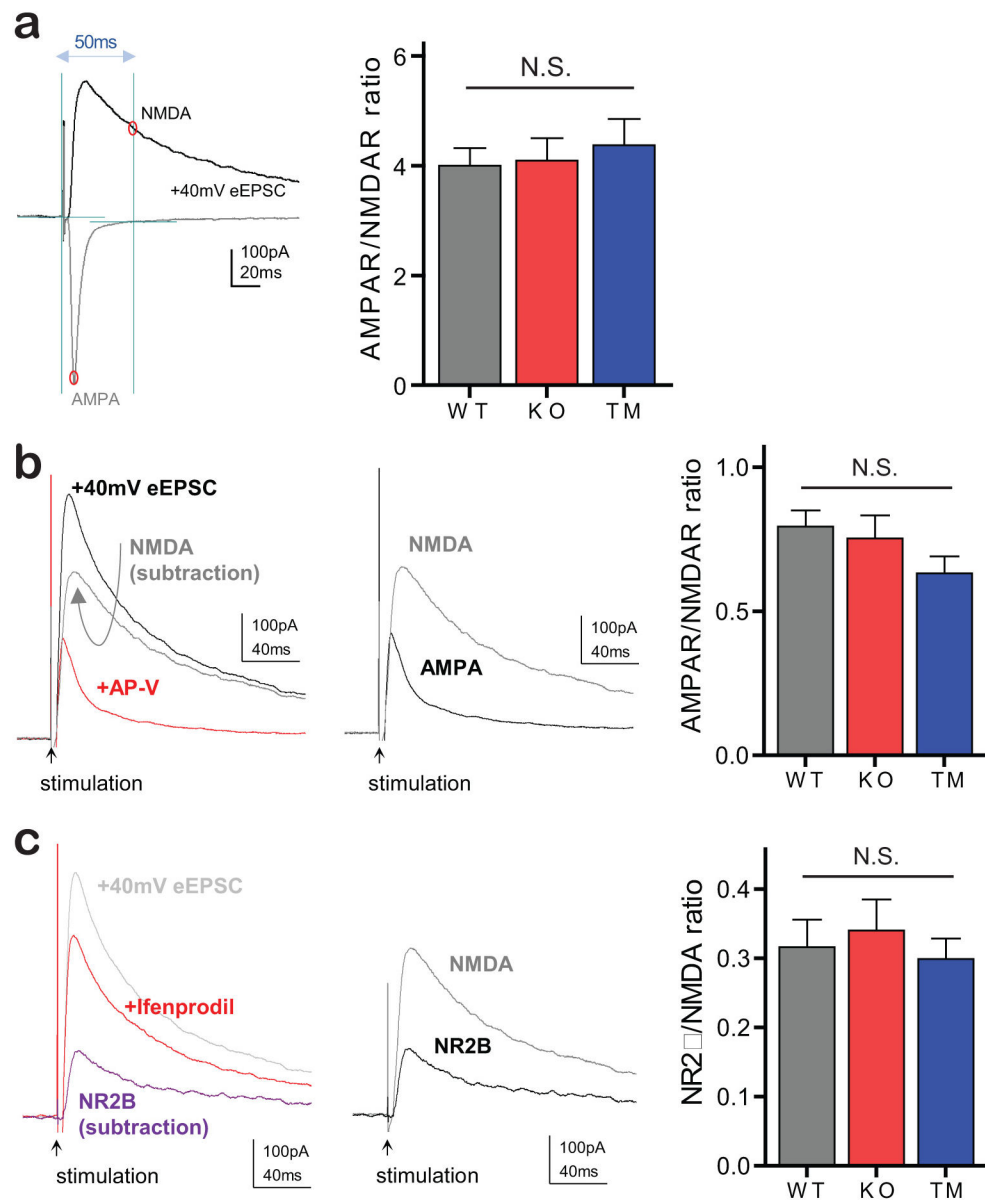
Extended Data Figure 2. Additional measurements of dorsal striatum synaptic function in tamoxifen rescue (TM)

a, Representative traces (left) and bar graph (right) for AMPAR/NMDAR ratio in WT, KO and TM groups (WT=30, KO=33, TM=33 MSNs). AMPAR/NMDAR ratio calculated as the ratio of the EPSC peak amplitude at 70 mV (AMPAR EPSC) to the amplitude of the EPSC recorded at +40 mV, 50 ms after afferent stimulation. **b**, Representative traces (left) and bar graph (right) for pharmacologically isolated AMPAR/NMDAR ratio (WT=20, KO=20,

TM=23 MSNs). Dual-component evoked EPSC at +40 mV recorded before and after APV bath application. **c**, Representative traces (left) and bar graph (right) for NR2B/NMDAR ratio in WT, KO and TM groups (WT=16, KO=16, TM=22 MSNs). Dual-component evoked EPSC at +40 mV recorded before and after ifenprodil bath application. Kruskal-Wallis test, with Dunn's multiple comparison test for **a**, one-way ANOVA Bonferroni post-hoc test for **b** and **c**. All data presented as means ± s.e.m.
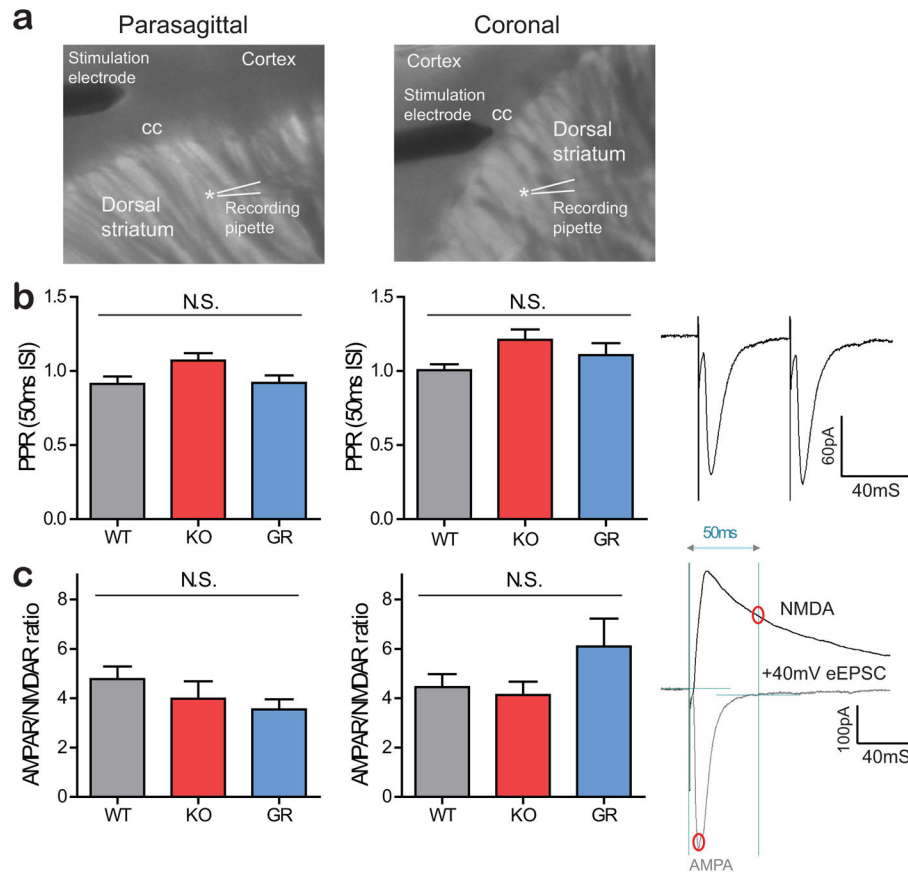
Extended Data Figure 3. Additional measurements of synaptic function in dorsal striatum by cortical and *corpus callosum* (cc) evoked stimulation (parasagittal and coronal slices respectively)
a, IR-DIC images showing representative placement of the stimulation electrode in the cortex (left) or corpus callosum (right) to evoke EPSCs in dorsal striatum using parasagittal (left) and coronal slices (right). **b**, Representative traces (right) and summary bar graphs for paired-pulse ratios (PPR) of evoked EPSCs in dorsal striatum MSNs, showing similar magnitude in parasagittal (left bar graph; WT=23, KO=20, TM=20 MSNs) and coronal slices (right bar graph; WT=9, KO=11, TM=10 MSNs). One-way ANOVA Bonferroni post-hoc test. **c**, Representative traces (right) and summary bar graphs of AMPAR/NMDAR ratios evoked in parasagittal (left bar graph; WT=17, KO=15, TM=16 MSNs) and coronal slices (right bar graph; WT=20, KO=16, TM=15 MSNs) from all 3 genotypes. AMPAR/NMDAR ratio calculated as the ratio of the EPSC peak amplitude at 70 mV (AMPAR EPSC) to the amplitude of the EPSC recorded at +40 mV, 50 ms after afferent stimulation (panel c, right

side). Kruskal-Wallis test, with Dunn's multiple comparison test. All data presented as means ± s.e.m.
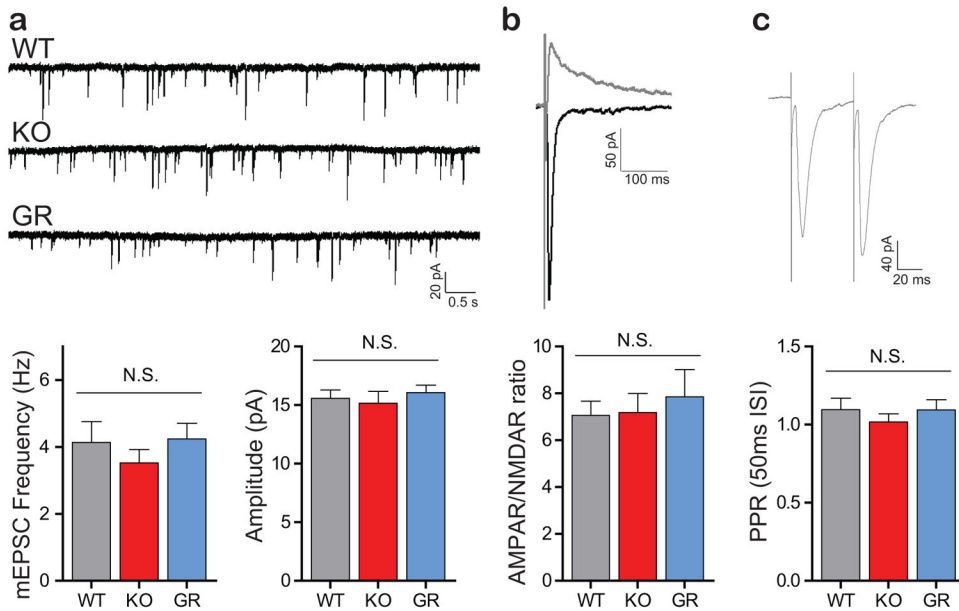
Extended Data Figure 4. Whole-cell measurements of excitatory synaptic function in nucleus accumbens (NAc)

a, Representative traces (top) and summary bar graphs (bottom) of mEPSCs in NAc-MSNs (WT=22, KO=16, GR=18 MSNs). **b**, Representative traces (top) and summary bar graph (bottom) of AMPAR/NMDAR ratio in NAc-MSNs. AMPAR/NMDAR ratio calculated as the ratio of the EPSC peak amplitude at 70 mV (AMPAR EPSC) to the amplitude of the EPSC recorded at +40 mV, 50 ms aft er afferent stimulation (WT=19, KO=16, GR=15 MSNs). **c**, Representative traces (top) and summary bar graph (bottom) of paired-pulse ratios in NAc-MSNs (WT=25, KO=22, GR=19 MSNs). One-way ANOVA Bonferroni post-hoc test for **a** and **c**, Kruskal-Wallis test, with Dunn's multiple comparison test for **b**. All data presented as means ± s.e.m.
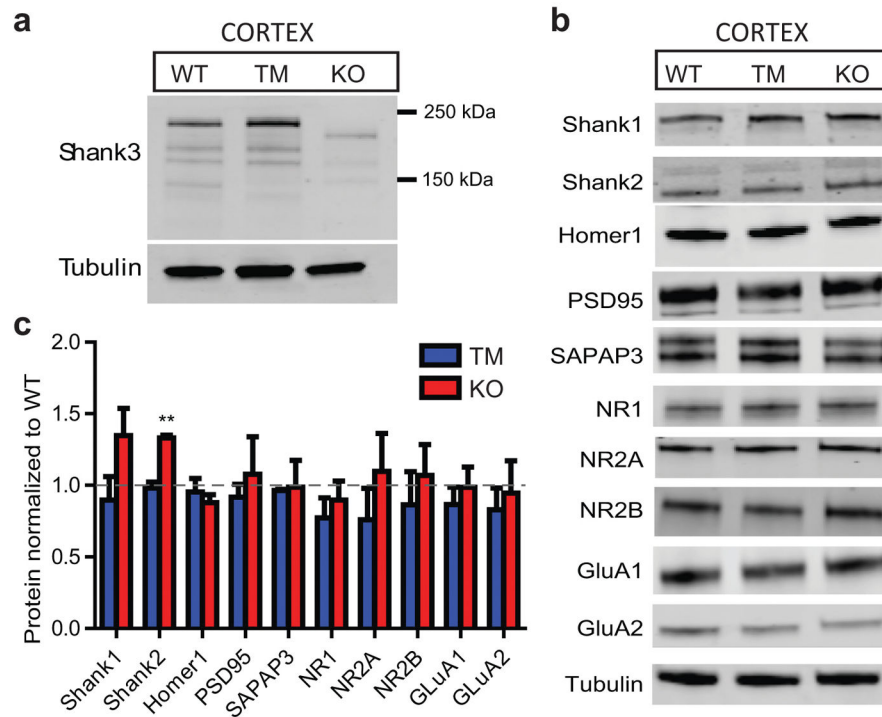
Extended Data Figure 5. Western blots of synaptosomal preparations from the cortex of the adult treated mice show minimal difference across genotypes

a, Representative Western blot on SHANK3 in the cortex of adult WT, KO and TM mice, showing that most major Shank3 isoforms are restored in the TM mice. **b**, Representative Western blots of synaptic proteins including scaffolding proteins and neurotransmitter receptors in the adult cortex across genotypes. **c**, Quantification of multiple synaptic proteins in the cortex of the adult treated mice. All data WT N=3, TM N=3, KO N=3; each sample is from tissue taken from two animals. Student's two-tailed unpaired t-test. All data presented as means ± s.e.m. See Supplementary Figure 1 for gel source data.
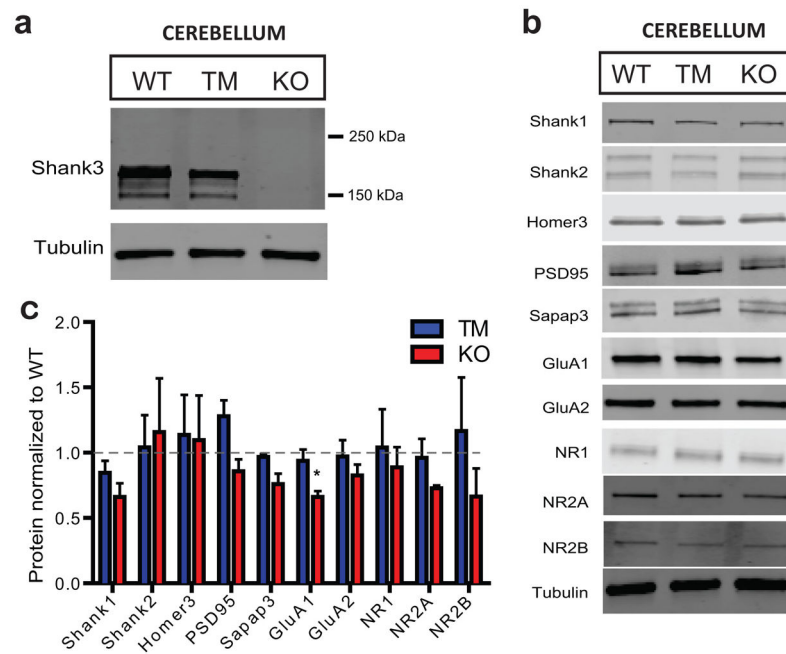
Extended Data Figure 6. Western blots of synaptosomal preparations from the cerebellum of the adult treated mice show minimal difference across genotypes

a, Representative Western blot of SHANK3 in the cerebellum of the adult mice treated with tamoxifen, showing that SHANK3 isoforms are restored in the TM mice. **b**, Representative Western blots of synaptic proteins in the adult cerebellum across genotypes. **c**, Quantification of multiple synaptic proteins in the cerebellum of the adult treated mice. All data WT N=3, TM N=3, KO, N=3; each sample is from tissue taken from a single animal. Student's two-tailed unpaired t-test. All data presented as means ± s.e.m. See Supplementary Figure 1 for gel source data.
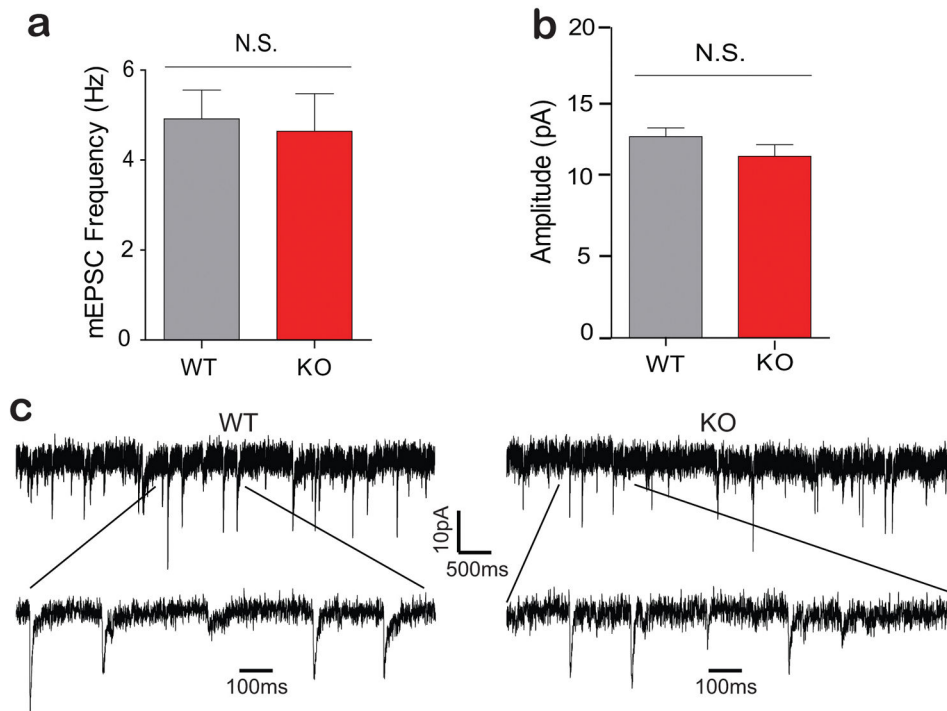
Extended Data Figure 7. Whole-cell measurements of excitatory synaptic function in the cortex
a, Summary bar graph of mEPSC frequency in the prefrontal cortex of the adult WT and KO. **b**, Summary bar graph of mEPSC amplitude in the prefrontal cortex of the adult WT and KO. **a,b,** WT N=13, KO N=10 cells; Student's two-tailed unpaired t-test. All data presented as means ± s.e.m. **c**, Representative traces from mEPSC recordings in the adult prefrontal cortex of the WT and KO.
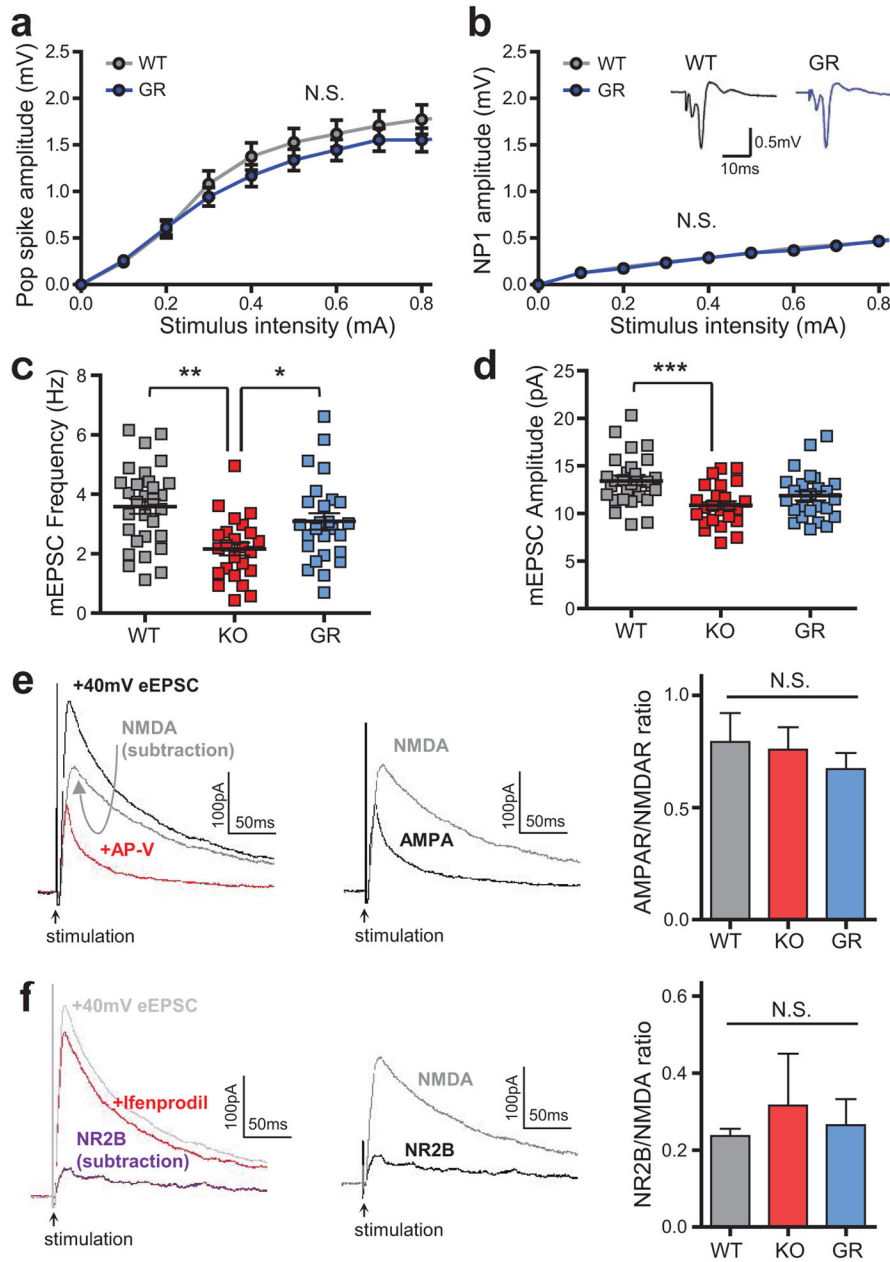
Extended Data Figure 8. Electrophysiological measurements in the dorsal striatum of germline rescue mice (GR)

a,**b**, Normal pop spike amplitude (a) and NP1 (b) in germline rescued (GR) mice (insets show representative field traces). **c,d**, Reduced mEPSC frequency in KO mice compared to WT and GR. A reduction in mEPSC peak current amplitude is observed between KO and WT group only (WT=30, KO=24, GR=26 MSNs). **e**, Representative traces (left) and bar graph (right) for pharmacologically isolated AMPAR/NMDAR ratio (WT=9, KO=9, GR=8 MSNs). Dual-component evoked EPSC at +40 mV recorded before and after APV bath application. **f**, Representative traces (left) and bar graph (right) for NR2B/NMDAR ratio in

WT, KO and GR groups (WT=6, KO=5, GR=7 MSNs). Dual-component evoked EPSC at +40 mV recorded before and after ifenprodil bath application.). Two-way ANOVA Bonferroni post-hoc test for **a** and **b**; one-way ANOVA Bonferroni post-hoc test for **c–f**. *$p<0.05$; **$p<0.01$; ***$p<0.001$ (ANOVA). Data are means ± s.e.m.
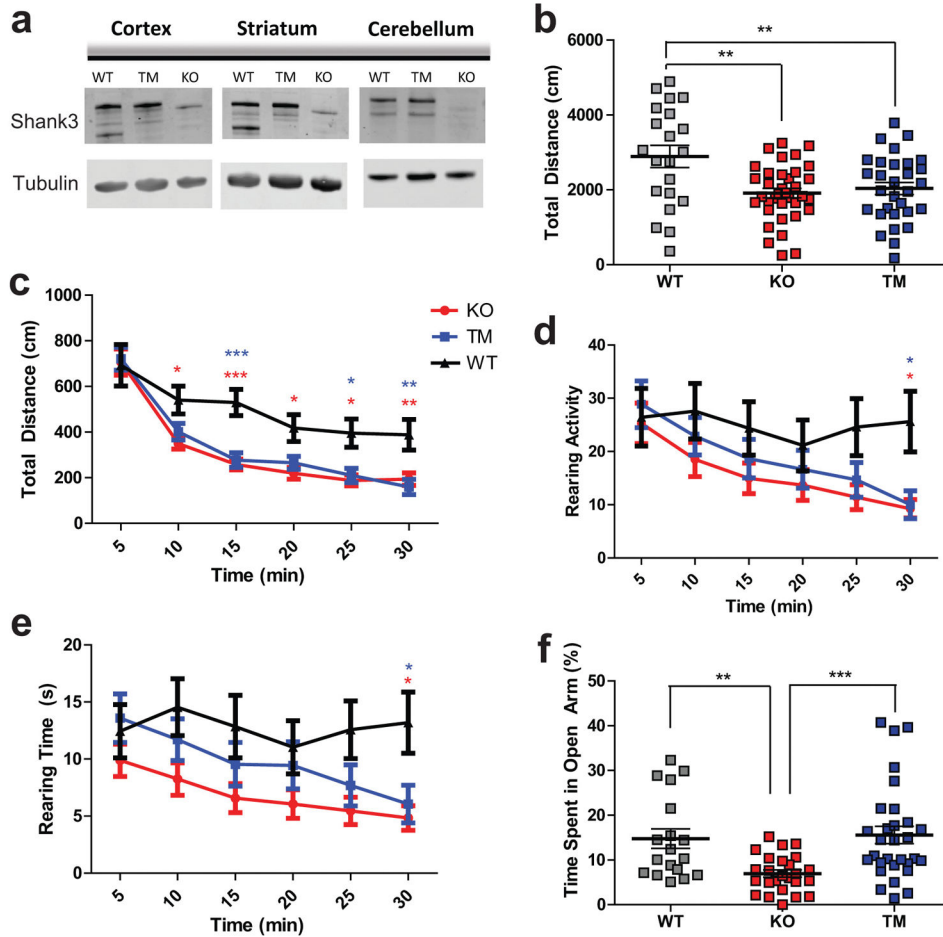
Extended Data Figure 9. Expression of Shank3 at P20–21 rescues some behavioral measurements
a, Representative Western blots showing efficient SHANK3 re-expression in the cortex, striatum, and cerebellum in mice that were treated with tamoxifen at P20–21. **b**, The total distance traveled as measured by the open field test was not improved in the tamoxifen condition compared to the KO condition. One-way ANOVA, Bonferroni post-hoc test. **c**, The open field total distance plotted across 5-minute time bins, showing that there is no difference between KO and TM conditions across time. **d.** Rearing activity measured by open field plotted across time, showing that TM mice perform in between WT and KO for most of the 30-minute test. **e.** Rearing time measured by open field plotted across time, also showing that the intermediate performance of TM between that of WT and KO. (**b** to **e**) WT N=21, KO N=36, TM N=30. Two-way ANOVA, Bonferroni post-hoc test. **f.** Activity on the zero maze indicates that the TM condition shows significantly reduced anxiety compared to that of the KO condition. WT N=18, KO N=25, TM N=30; outliers were removed using

Iglewicz and Hoaglin's test (two-sided); Kruskal-Wallis test, Dunn's Multiple Comparison test. All data presented as means ± s.e.m. See Supplementary Figure 1 for gel source data.
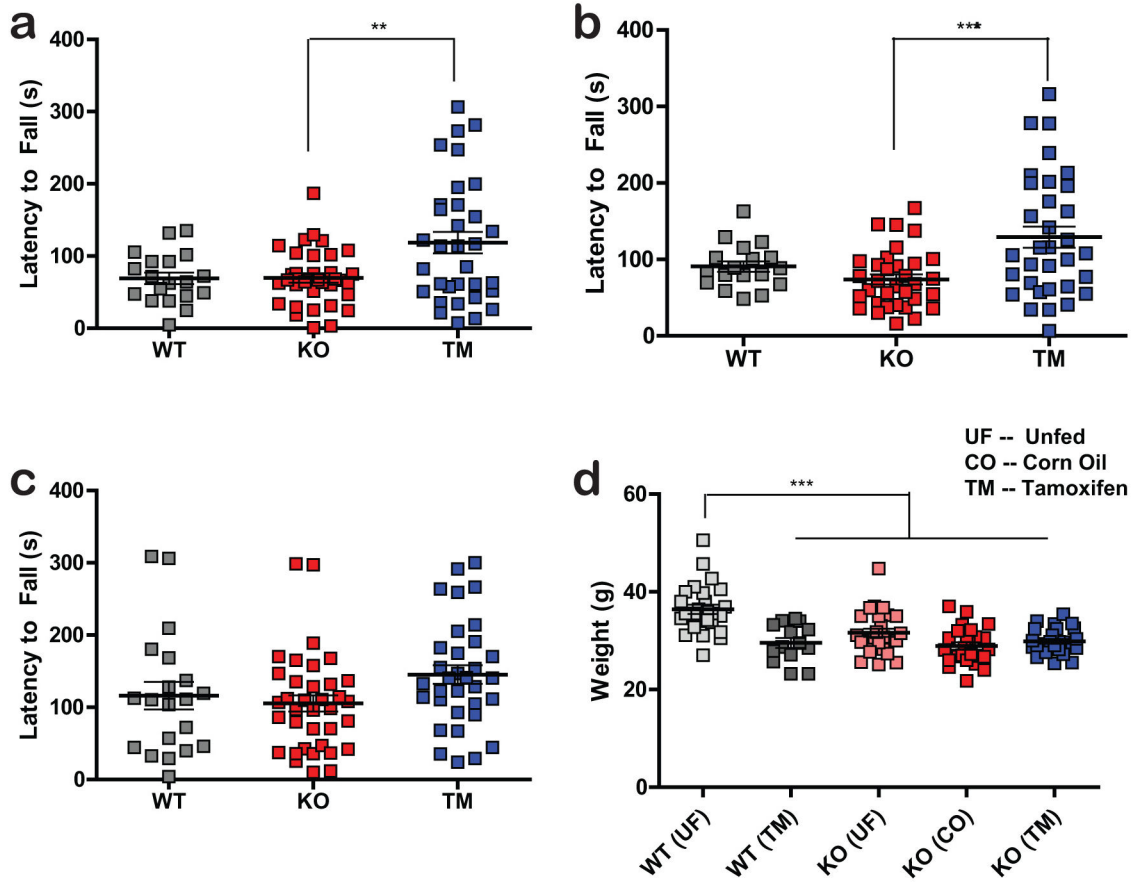
Extended Data Figure 10. Expression of Shank3 at P20–21 improves motor coordination
a, Summary data from trial 1 of the accelerating rotarod test on mice treated with TM at P20–21. WT N=19, KO N=35, TM N=33. **b**, Summary data from trial 2 of the same rotarod test on mice treated at P20–21. WT N=18, KO N=33, TM N=33. **c**, Summary data from trial 3 of the rotarod on mice treated at P20–21. WT N=20, KO N=36, TM N=33. **a–c,** Outliers were removed using Iglewicz and Hoaglin's robust outlier test. One-way ANOVA, Bonferroni post-hoc test. **d,** Body weight from WT and KO that were unfed (UF) and mice that were fed with either corn oil or TM. WT(UF) N=28, WT(TM) N=14, KO(UF) N=27, KO(CO) N=25, KO (TM) N=26; One-way ANOVA, Bonferroni post-hoc test. All data presented as means ± s.e.m.

Supplementary Material

Refer to Web version on PubMed Central for supplementary material.

Acknowledgments

References

1. Amaral, D.; Geschwind, D.; Dawson, G., editors. Autism Spectrum Disorders. 1. Oxford University Press; 2011.

2. Gauthier JD, et al. Novel de novo SHANK3 mutation in autistic patients. Am J Med Genet Part B Neuropsychiatr Genet. 2009; 150:421–424.

3. El-Fishawy P, State MW. The genetics of autism: key issues, recent findings, and clinical implications. Psychiatr Clin North Am. 2010; 33:83–105. [PubMed: 20159341]

4. Leblond CS, et al. Meta-analysis of SHANK Mutations in Autism Spectrum Disorders: A Gradient of Severity in Cognitive Impairments. PLoS Genet. Sep.2014 10(9):e1004580. [PubMed: 25188300]

5. Moessner R, et al. Contribution of SHANK3 mutations to autism spectrum disorder. Am J Hum Genet. 2007; 81:1289–1297. [PubMed: 17999366]

6. Durand M, et al. Mutations in the gene encoding the synaptic scaffolding protein SHANK3 are associated with autism spectrum disorders. Nat Genet. 2007; 39:25–27. [PubMed: 17173049]

7. Ebert DH, Greenberg ME. Activity-dependent neuronal signalling and autism spectrum disorder. Nature. 2013; 493:327–37. [PubMed: 23325215]

8. Kim E, et al. GKAP, a novel synaptic protein that interacts with the guanylate kinase- like domain of the PSD-95/SAP90 family of channel clustering molecules. J Cell Biol. 1997; 136:669–678. [PubMed: 9024696]

9. Takeuchi M, et al. SAPAPs. A family of PSD-95/SAP90-associated proteins localized at postsynaptic density. J Biol Chem. 1997; 272:11943–11951. [PubMed: 9115257]

10. Wang X, et al. Synaptic dysfunction and abnormal behaviors in mice lacking major isoforms of Shank3. Hum Mol Genet. 2011; 20:3093–3108. [PubMed: 21558424]

11. Bozdagi O, et al. Haploinsufficiency of the autism-associated Shank3 gene leads to deficits in synaptic function, social interaction, and social communication. Mol Autism. 2010; 1:15. [PubMed: 21167025]

12. Peça J, et al. Shank3 mutant mice display autistic-like behaviours and striatal dysfunction. Nature. Apr; 2011 472(7344):437–42. [PubMed: 21423165]

13. Yang M, et al. Reduced Excitatory Neurotransmission and Mild Autism-Relevant Phenotypes in Adolescent Shank3 Null Mutant Mice. J Neurosci. 2012; 32:6525–6541. [PubMed: 22573675]

14. Sheng M, Kim E. The Shank family of scaffold proteins. J Cell Sci. Jun; 2000 113(Pt 1):1851–6. [PubMed: 10806096]

15. Boeckers TM, et al. Proline-rich synapse-associated proteins ProSAP1 and ProSAP2 interact with synaptic proteins of the SAPAP/GKAP family. Biochem Biophys Res Commun. Oct; 1999 264(1): 247–52. [PubMed: 10527873]

16. Han K, et al. SHANK3 overexpression causes manic-like behaviour with unique pharmacogenetic properties. Nature. 2013; 503:72–7. [PubMed: 24153177]

17. Schnütgen F, et al. A directional strategy for monitoring Cre-mediated recombination at the cellular level in the mouse. Nature Biotechnology. 2003

18. Karayannis T, et al. Cntnap4 differentially contributes to GABAergic and dopaminergic synaptic transmission. Nature. 2014

19. Guo C, Yang W, Lobe CG. A Cre recombinase transgene with mosaic, widespread tamoxifen-inducible action. Genesis. 2002; 32:8–18. [PubMed: 11835669]

20. Rothwell PE, et al. Autism-associated neuroligin-3 mutations commonly impair striatal circuits to boost repetitive behaviors. Cell. 2014; 158:198–212. [PubMed: 24995986]

21. Welch JM, et al. Cortico-striatal synaptic defects and OCD-like behaviours in Sapap3-mutant mice. Nature. Aug; 2007 448(7156):894–900. [PubMed: 17713528]

22. Chao H-T, et al. Dysfunction in GABA signalling mediates autism-like stereotypies and Rett syndrome phenotypes. Nature. 2010; 468:263–269. [PubMed: 21068835]

23. Dolen G, et al. Social reward requires coordinated activity of nucleus accumbens oxytocin and serotonin. Nature. 2013; 501:179–184. [PubMed: 24025838]

24. Gross C, et al. Serotonin1A receptor acts during development to establish normal anxiety-like behaviour in the adult. Nature. 2002; 416:396–400. [PubMed: 11919622]

25. De Zeeuw CI, Ten Brinke MM. Motor learning and the cerebellum. Cold Spring Harbor Perspectives in Biology. 2015 Sep 1.7(9) Review.

26. Poirier MC, Schild LJ. The genotoxicity of tamoxifen: extent and consequences, Kona, Hawaii, January 23, 2003. Mutagenesis. 2003 Jul; 18(4):395–9. [PubMed: 12840114]

27. Guy J, Gan J, Selfridge J, Cobb S, Bird A. Reversal of neurological defects in a mouse model of Rett syndrome. Science. 2007; 315:1143–1147. [PubMed: 17289941]

28. Clement JP, et al. Pathogenic SYNGAP1 mutations impair cognitive development by disrupting maturation of dendritic spine synapses. Cell. 2012; 151:709–723. [PubMed: 23141534]

29. Hancock JF, Cadwallader K, Paterson H, Marshall CJ. A Caax or a Caal Motif and a 2nd Signal are sufficient for plasma-membrane targeting of Ras proteins. Embo Journal. 1991; 10(13):4033–4039. [PubMed: 1756714]
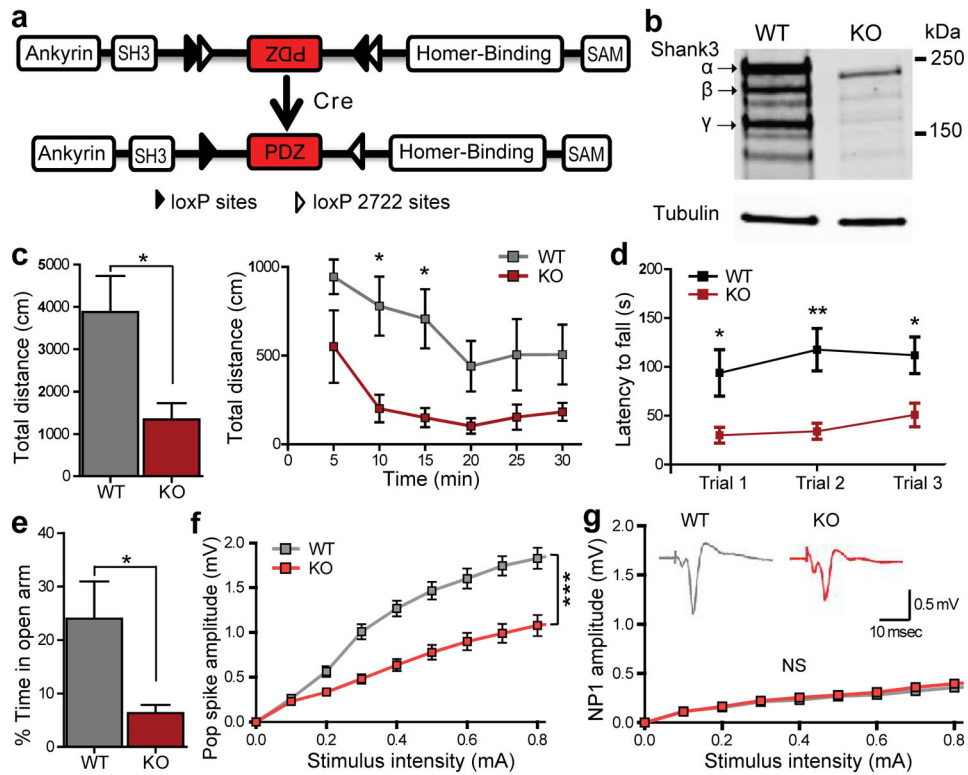
Figure 1. *Shank3*^{fx/fx} mice have deficits in neurotransmission and behavior

a, Domain structure of SHANK3 protein, with FLExed PDZ domain inverted, which can be re-oriented in the presence of Cre. **b**, Western blot showing *Shank3* expression in striatal PSD from wildtype (WT) and *Shank3*^{fx/fx} (KO) mice. **c**, KO mice show decreased total distance traveled in the open field test compared to WT. **d**, KO mice show impaired motor coordination in rotarod test. **e**, KO mice spend less time in the open arm in elevated zero maze test. **f**, KO mice show decreased pop spike amplitude in extracellular field recordings in the striatum. **g**, Normal relationship of stimulation intensity to the negative peak 1 amplitude (NP1; action potential component) suggesting unaltered presynaptic function; insets show representative traces. *$P < 0.05$, **$P<0.01$, ***$P< 0.001$; all data presented as means ± s.e.m. (all behavior data from n=6 WT and n=7 KO mice); two-tailed *t*-test for **c** (left panel) and **e**; two-way repeated measures ANOVA with Bonferroni *post hoc* test for **c** (right panel), **d**, **f** and **g** (electrophysiology data from n=9 slices; 3 mice *per* genotype). See Supplementary Figure 1 for gel source data.
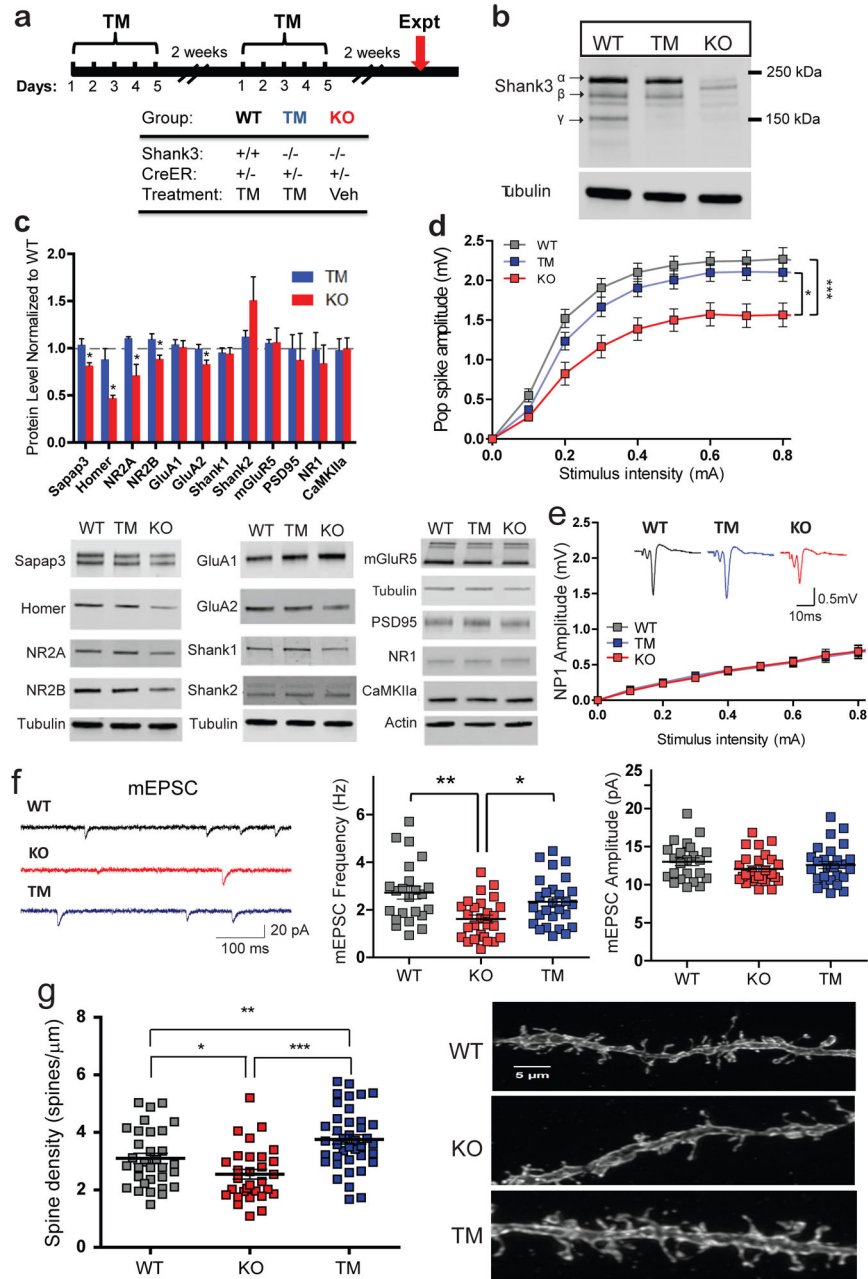
Figure 2. Rescue of PSD proteins and striatal neurotransmission
a, Experimental groups and TM feeding scheme. **b**, Western blot from striatal synaptosome preparation after tamoxifen feeding (TM) shows restoration of most SHANK3 isoforms. **c**, Western blots of striatal synaptosomal fractions; PSD protein levels in KO mice are restored to WT levels in TM group. **d**, Striatal field response in KO mice was rescued in TM mice. **e**, Representative traces for WT, KO and TM mice. Indistinguishable relationship of stimulation intensity to the NP1 amplitude among groups suggests unaltered presynaptic function. **f,** Rescued mESPC frequency in the striatum in the TM compared to the KO. **g,** Increased spine density in the TM compared to the KO, while spine density in the KO is

lower than that of the WT. *P< 0.05, **P<0.01, ***P< 0.001; all data presented as means ± s.e.m. Student's two-tailed *t*-test for **c** (n=3 WT, n=4 TM, n=3 KO; each sample represents combined striatal tissue from 2 mice); Two-way repeated measures ANOVA, with Bonferroni *post hoc* test for **d** and **e** (n=12 slices from 4 WT, n=12 slices from 4 TM and n=12 slices from 4 KO mice). One-way ANOVA with Bonferroni *post hoc* test for **f** (n=23 cells for WT, n=26 cells for KO, and n=27 cells for TM). One-Way ANOVA, Newman-Keuls Multiple Comparison test for **g** (n=32 dendritic segments for WT, n=30 for KO, and n=40 for TM). See Supplementary Figure 1 for gel source data.
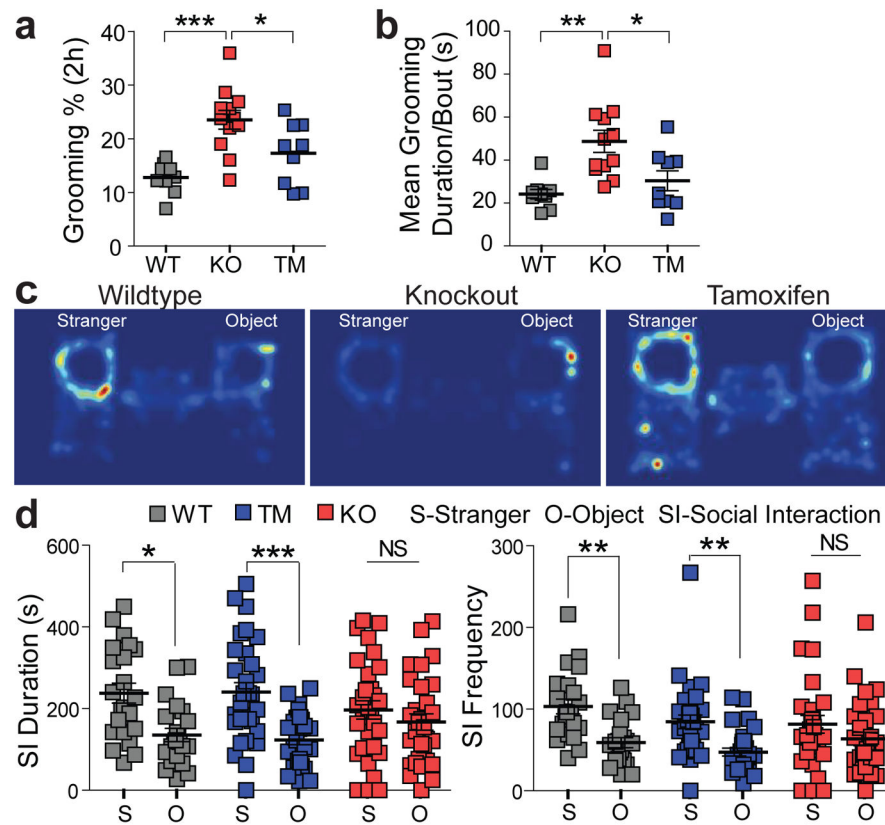
Figure 3. Adult *Shank3* expression rescued repetitive grooming and social interaction
a,b, Significantly reduced repetitive grooming behavior in TM mice compared to KO mice.
c, Representative heat maps from the social interaction test for all groups. **d,** Unlike WT mice, KO mice showed no preference for interaction with a stranger mouse; this behavior is rescued in TM group. *P<0.05, **P<0.01, ***P<0.001; all data presented as means ± s.e.m; one-way repeated measures ANOVA with Bonferroni *post hoc* test for **a,b** (n=9 WT, n=9 TM and n=12 KO mice). Social interaction duration data (d, left panel) was analyzed using one-way repeated measures ANOVA with Bonferroni *post hoc* test. Social interaction frequency data (d, right panel) was analyzed using Kruskal-Wallis test with Dunn's multiple comparison test due to the distribution not being normally distributed (n=22 WT, n=30 TM and n=30 KO).
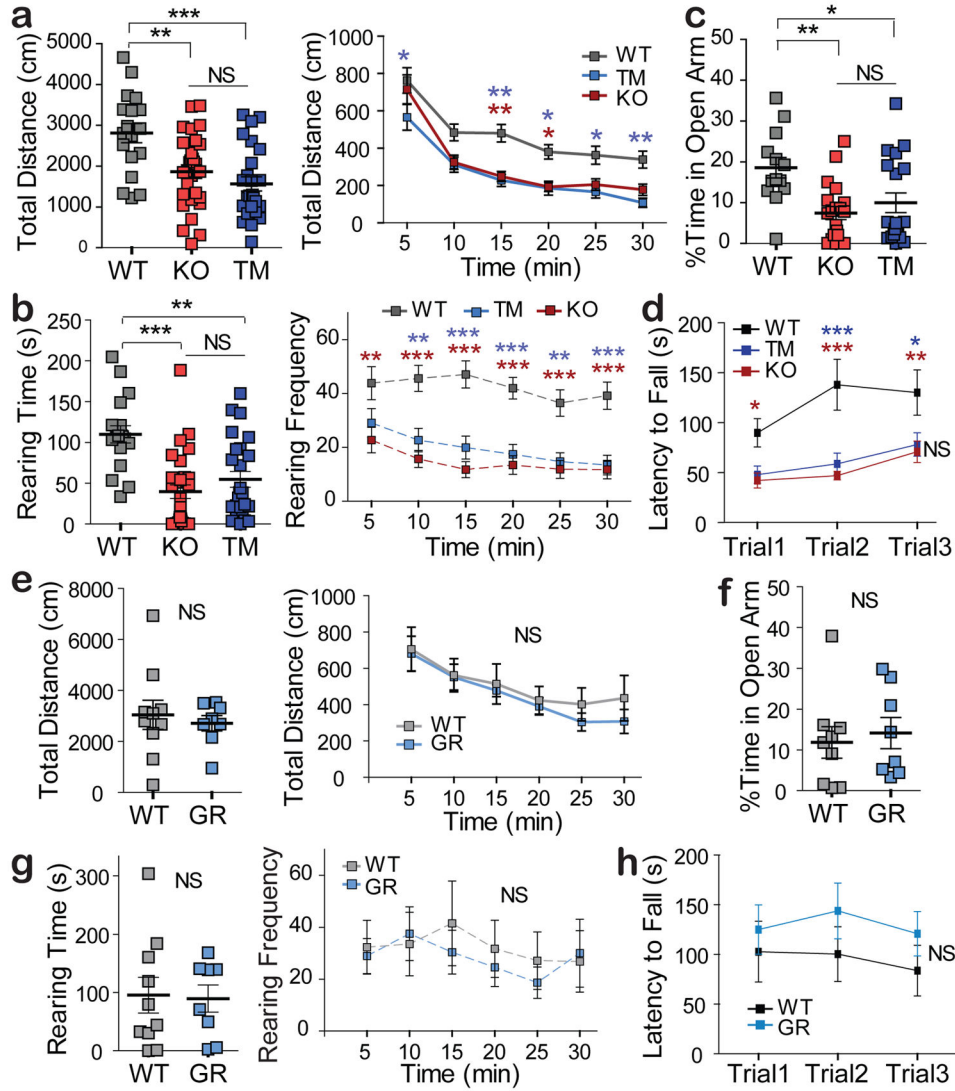
Figure 4. Restoring *Shank3* expression in adulthood did not rescue anxiety and rotarod deficits
a,b, Open field tests indicated that Shank3 re-expression in adults (TM) does not rescue reduced locomotion and reduced rearing (axiogenic behavior) in KO mice. **c**, KO mice spend less time exploring the open arm in elevated zero maze test; this behavior is also not rescued in TM group. **d**, Motor coordination measurement from rotarod is not rescued in TM group. **e–h**, Germline rescued *Shank3^(fx/fx)* mice (GR) show that all above parameters for open field, elevated zero maze and rotarod tests can be rescued if *Shank3* expression is restored at germ cell stage. *P < 0.05, **P<0.01, ***P < 0.001; One way ANOVA for **a** (left panel), **c**; Kruskal-Wallis test with Dunn's multiple comparisons for **b** (left panel). Two-tailed *t*-test for **e** (left panel), **f** and **g** (left panel); Two-way repeated measures ANOVA with Bonferroni *post hoc* test for **a** (right panel), **b** (right panel), **d**, **e** (right panel), **g** (right panel) and **h**; All data presented as means ± s.e.m. (**a–c**: n=18 WT, n=25 TM and n=27 KO; **d**: n=13 WT, n=19 TM and n=21 KO; **e–h**: n=10 WT and n=8 GR mice).